Centroid distortion of a wavefront with varying amplitude due to asymmetry in lens diffraction

Yuval Carmon[1,2] and Erez N. Ribak[1]

[1]Department of Physics, Technion – Israel Institute of Technology,

Haifa 32000, Israel

[2]Shamir Optical Industry, Shamir, Upper Galilee 12135, Israel

It is often if interest to measure the centroid of a light intensity pattern in order to deduce physical properties. Examples are the Hartmann-Shack sensor, which measures the wavefront slopes, and position sensors. We investigate whether amplitude changes of the incoming electromagnetic field can affect the location of the centroid and we show that the effect is strongly dependent on the relative size of the diffraction pattern in relation to the lenslet size. We show that if the phase varies slowly in space, and the focal spot size relative to the centroid integration area approaches zero – this variation does not affect the centroid. This is a consequence of symmetry properties of the Fresnel operator. We then show that when the focal width is not infinitely small, changes in the field amplitude can exacerbate distortion of the centroid results.

OCIS: 010.7350, 010.1080, 330.4300, 260.1960

1. Introduction

Wave front sensors (WFSs) were developed to measure the quality of optical components during manufacture. The first WFSs were interferometers, and indeed soon applied in astronomy [1, 2]. In ocular WFSs the source, usually coherent light scattered off the retina, is too unsteady and speckled to make interferometry practical. Other, non-interferometric WFSs can be used for measuring the wave front instead, such as pyramid sensors, curvature sensors or Hartmann-Shack sensors (HSSs) [1]. The wave front thus measured can then be used for optical correction of the wavefront using adaptive optics. This enables getting images in which finer detail becomes apparent. The HSS is the most common of these WFSs because of its ease of use and intuitive appeal.

The HSS is composed of an array of small lenslets that dissect the wavefront into many small subapertures. A CCD is placed at the image plane of these lenslets. The average wavefront gradient over the aperture is the stray of the spot location on the detector plane divided by the lenslet focal length. This gradient field can then be integrated using different methods to yield the wave front [3 - 7]. So the underlying assumption in the HSS is that the wavefront changes slowly enough over each subaperture, that discarding higher order derivatives from the measurement does not affect the accuracy of the reconstructed wavefront.

There are many ways to analyze the HSS image [8 - 10], and derive from it the gradient field of the wave front. Some of them derive from the known shape of the diffraction spot, to provide a matched filter of some sort [11]. The most commonly used is the centroiding method, being simple and fast, e.g. for ocular purposes [12,13]. Using this method, the detector (usually a CCD) is divided into many subsections, each assigned to contain a single lenslet focal spot. We will refer henceforth to this division of the CCD as a tiling, and to each of these subsections as a tile. Within each tile, the center of mass of the intensity is calculated. Its location is found relative to where it would have been, had a perfectly planar wavefront been measured with the same sensor. The spot pattern of a planar beam is often measured independently and used as a reference.

It has been shown that a key parameter for describing the fidelity of the HSS is the relation between the decay width of each diffraction pattern and the width of the associated tile. The smaller this value is, the higher the performance of the HSS (up to where the detector pixels are comparable in size to the spot width). We will refer to this henceforth as the duty cycle. Because some of the photons stray out of the tile, a bias is introduced towards the center of the tile [10]. This causes distortion in the centroid analysis of each lenslet. This phenomenon becomes progressively worse as the duty cycle increases. In addition, the interference between Fresnel diffraction patterns of neighboring lenslets in a HSS [14] has been shown to become more dominant as the duty cycle increases, thus causing further deterioration in the fidelity of the HSS in high duty cycles.

In many cases the amplitude of the electromagnetic (EM) field across the whole aperture or within one subaperture is not constant. For example, scintillation due to middle-range turbulence in astronomy [15], dirty optics, defective detector sections, etc. In ocular wave front measurements it is well known that the back-scatter of a point source on the retina is not constant across the whole pupil (the reverse Stiles-Crawford effect). Inhomogeneities floating in the aqueous humor of the eye cause intensity variations, and polarization effects can also potentially change

the EM amplitude. Laser beams also intrinsically exhibit this behavior having a Gaussian amplitude [16,17]. Bara [18] has analyzed the effect a non-constant EM amplitude would have on the measurement of a wavefront using a HSS sensor and the centroiding method. The effect on the centroid operator and on the induced reconstructed wave front was discussed; it was shown that varying amplitude exacerbates the distortion of the centroid operator. Following Teague [19], the moments of the optical intensity function at the image plane were calculated using the phase and amplitude of the optical wave at the aperture plane. Using this approach the centroid can only be calculated over the whole image plane, and not over a finite area. So implicitly the duty cycle was assumed to be zero. It is of interest to investigate this problem again, but this time using techniques that enable calculating the centroid over a finite area, using a finite duty cycle.

In what follows we will analyze the first moment of a Fresnel diffraction pattern at the image plane of a wave passing through an aperture whose phase changes slowly in space, an assumption intrinsic to the HSS sensor. In the first section, we will formulate the value of the distortion of the centroid operator, and we will show that when the duty cycle approaches zero, the amplitude and aperture shape do not cause distortion to the centroid operator at all. This is easily understood when one analyzes the symmetry properties of the Fresnel operator with relation to the parity operator $\Pi : f(\overline{r}) = f(-\overline{r})$.

In the second section, we will investigate the distortion of the centroid operator caused by a nonuniform amplitude when the duty cycle is finite. There we will assume that both phase and amplitude change slowly enough so that we can approximate them both as piecewise planes over the aperture plane. In effect we are adding a perturbation to the customary model of the HSS in which the amplitude is assumed to be constant, and investigating the repercussions. The addition of a term that is not constant in amplitude will be shown to contribute a new term to the Fresnel diffraction pattern. We will show that the distortion of the first moment is exacerbated relative to the constant amplitude case [10]. Moreover, when the amplitude is constant, the induced bias can easily be compensated for in the centroiding operator. But when the term of variable amplitude is added, compensation becomes impractical as the compensation bias depends on the amplitude gradient size and direction over each subaperture. Compensating for this effect would be costly in computation time for real time applications such as adaptive optics. Since our analysis is performed for a lens in general, it applies both to position sensors and to HSS. Thus issues such as the sampling

density of the wavefront, or cross talk between lenslets, are beyond this analytical calculation, and are dealt with elsewhere [1, 3-5, 14, 18].

2. Centroid operator of a wavefront with spatially slow phase, at zero duty cycle

We start with the Fresnel integral for the complex EM field at the image plane of the lens:

$$U(x,y)=\gamma\int_{-\infty}^{\infty}\int_{-\infty}^{\infty}U(x_1,y_1)\exp[-i\alpha(xx_1+yy_1)]\,dx_1dy_1 \quad . (1)$$

Here $\alpha = 2\pi/\lambda f$, and $\gamma=(\lambda f)^{-1}\exp(i\alpha f^2)\exp(i\alpha r^2/2)$. We will be using $\bar{r}=(x,y)$, $\bar{r}_1=(x_1,y_1)$, $r=(x^2+y^2)^{1/2}$ and $r_1=(x_1^{\,2}+y_1^{\,2})^{1/2}$ interchangeably. Coordinates without a subscript signify location in the image plane and a subscript of 1 signifies location in the aperture plane. Fig. 1 shows a schematic sketch of the physical system.

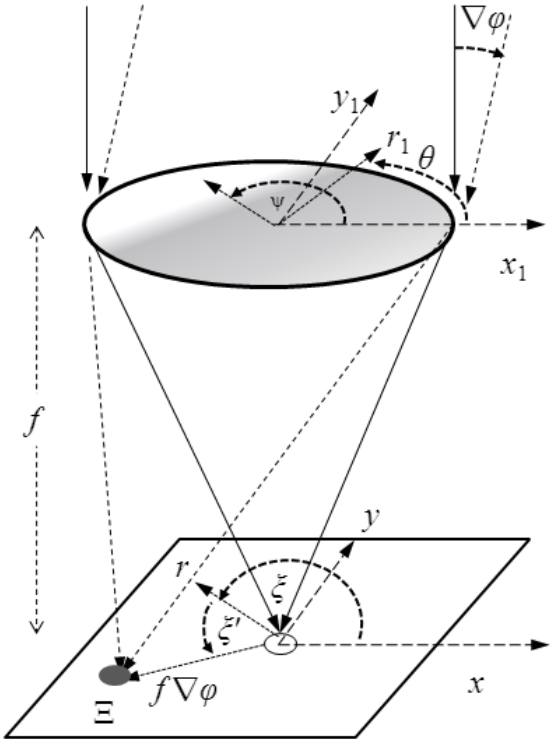

Fig. 1: Schematic sketch of the aperture plane and the image plane of a single lenslet.

The first order Taylor approximation for the phase of the EM field is $\varphi(\bar{r}_1) \approx \varphi_0 + \nabla\varphi \cdot \bar{r}_1$. The expansion is around the center of each lenslet subaperture. Since this form of the Fresnel operator can be viewed as a Fourier transform, one may now use the convolution theorem and write $U(\bar{r}) = U_1(\bar{r}) \otimes U_2(\bar{r})$. Here

$U_1(\bar{r}) = \gamma \int_{-\infty}^{\infty}\int_{-\infty}^{\infty} P(\bar{r}_1) A(\bar{r}_1) exp(-i\alpha\bar{r} \cdot \bar{r}_1) d\bar{r}_1$, with $P(\bar{r}_1)$ being the pupil function of the HSS lenslet and $A(\bar{r}_1)$ being the amplitude of the EM field arriving at the aperture. The second term of the convolution,

$U_2(\bar{r}) = \int_{-\infty}^{\infty}\int_{-\infty}^{\infty} exp[ik(\varphi_0 + \nabla\varphi \cdot \bar{r}_1)] exp(-i\alpha\bar{r} \cdot \bar{r}_1) d\bar{r}_1$, is proportional to a delta function:

$U_2(\bar{r}) = \left(e^{i\varphi_0}/\alpha^2\right)\delta(\bar{r} - f\nabla\varphi)$. Therefore the total diffraction pattern is in effect the Fresnel diffraction pattern of a wave with zero phase gradient rigidly translated by a vector that is proportional to the gradient of the phase $U(\bar{r}) = U_1(\bar{r} - f\nabla\varphi)$. $U_1(\bar{r}_1) = P(\bar{r}_1) A(\bar{r}_1)$ is a real function. Therefore its propagated EM field in the image plane (which is closely related to its Fourier transform as seen above) is a Hermitian function. So

$$\begin{aligned} &U_1(\bar{r}) = U_1^*(-\bar{r}) \\ &\mathcal{R}e\{U_1(\bar{r})\} = \mathcal{R}e\{U_1(-\bar{r})\} \\ &Im\{U_1(\bar{r})\} = -Im\{U_1(-\bar{r})\} \end{aligned} \quad (2),$$

where * denotes a conjugate complex operator, $\mathcal{R}e$ and Im signify the real and imaginary parts operators. Thus we have $U_1(\bar{r}) = U_1^{\,S}(\bar{r}) + iU_1^{\,AS}(\bar{r})$ where $U_1^{\,S}(\bar{r})$ and $U_1^{\,AS}(\bar{r})$ are symmetrical and anti-symmetrical with respect to the parity operator Π. Thus we can now write

$$\begin{aligned} &U(\bar{r}) = U_1^{\,S}(\bar{r} - f\nabla\varphi) + iU_1^{\,AS}(\bar{r} - f\nabla\varphi) \\ &I(\bar{r}) = \left[U_1^{\,S}(\bar{r} - f\nabla\varphi)\right]^2 + \left[U_1^{\,AS}(\bar{r} - f\nabla\varphi)\right]^2 \end{aligned}, \quad (3)$$

so overall $I(\bar{r})$ is symmetrical around an origin at $f\nabla\varphi$.

The centroid operator in a region Ξ is given by $\langle\bar{r}\rangle = \iint_\Xi \bar{r} I d^2r \Big/ \iint_\Xi I d^2r$. This can also be written as

$$\begin{aligned} \langle\bar{r}\rangle &= f\nabla\varphi + \iint_\Xi (\bar{r} - f\nabla\varphi) I d^2r \Big/ \iint_\Xi I d^2r \\ &= f\nabla\varphi + \bar{\Delta}_\Xi \end{aligned}. \quad (4)$$

Here $\overline{\Delta}_{\Xi}=\left(I_0^{\Xi}\right)^{-1}\iint_{\Xi}(\overline{r}-f\nabla\varphi)Id^2r$, and $I_0^{\Xi}=\iint_{\Xi}Id^2r$.

In the case of the HSS, Ξ is the region representing a single tile on the CCD. $\overline{\Delta}_{\Xi}$ signifies the distortion introduced by the fact that the amplitude, the integration range and the aperture are arbitrary. This value is also useful for calculating the distortion of the centroid operator when the duty cycle is finite, as we will see in the next sections.

We now show that as the duty cycle approaches zero, $\overline{\Delta}_{\Xi}$ approaches zero. We rewrite $\overline{\Delta}_{\Xi}$ as an integral over the whole real plane:

$$\begin{aligned}\overline{\Delta}_{\Xi}&=\left(I_0^{\Xi}\right)^{-1}\iint_{\Xi}(\overline{r}-f\nabla\varphi)Id^2r\\&=\left(I_0^{\Xi}\right)^{-1}\iint_{\mathbb{R}^2}A_{\Xi}(\overline{r}-f\nabla\varphi)Id^2r\end{aligned}$$

where

$$A_{\Xi}(\overline{r})=\begin{Bmatrix}1 & \overline{r}\in\Xi\\0 & \overline{r}\notin\Xi\end{Bmatrix}$$

is the support of the integral. Let us assume that the integration region is contiguous, and symmetrical around the *z* axis. We write the support in the following way:

$$A_{\Xi}=\left[A_{\Xi}-A_{(\Xi-f\nabla\varphi)}\right]+A_{(\Xi-f\nabla\varphi)},$$

where $A_{(\Xi-f\nabla\varphi)}(\overline{r})=A_{\Xi}(\overline{r}+f\nabla\varphi)$ is a symmetrical function around $f\nabla\varphi$. Because of the symmetry properties of I discussed above, the term $\left(I_0^{\Xi}\right)^{-1}\iint_{\mathbb{R}^2}A_{A_{(\Xi-f\nabla\varphi)}}(\overline{r}-f\nabla\varphi)Id^2r$ vanishes for any Ξ, regardless of the duty cycle. So we are left with $\overline{\Delta}_{\Xi}=\left(I_0^{\Xi}\right)^{-1}\iint_{\mathbb{R}^2}\left[\left(A_{\Xi}-A_{\Xi-f\nabla\varphi}\right)\right](\overline{r}-f\nabla\varphi)Id^2r$. We notice that

$$A_{\Xi}(\overline{r})-A_{\Xi-f\nabla\varphi}(\overline{r})=\begin{Bmatrix}1 & \overline{r}\in\Xi\setminus(\Xi-f\nabla\varphi)\\-1 & \overline{r}\in(\Xi-f\nabla\varphi)\setminus\Xi\\0 & otherwise\end{Bmatrix}\quad(5).$$

Here \ signifies the set complement operator. A schematic drawing of $A_{\Xi}(\bar{r}) - A_{\Xi - f\nabla\varphi}(\bar{r})$ is shown in Fig. 2. Now the integral has an effective support that is comprised of the difference between two support functions. For finite Ξ the expression is usually not zero and its behavior will be investigated in the next section. To study the behavior of $\bar{\Delta}_{\Xi}$ as the duty cycle approaches zero, we perform $\lim_{\Xi \to \mathbb{R}^2} \bar{\Delta}_{\Xi}$. As can be seen from Eq. (5) and Fig. 2, the only contribution to the integral comes from a range around the edge of the integration area, whose width is approximately $f\nabla\varphi$. As Ξ becomes larger, the intensity function approaches zero around the edges of Ξ until at the limit, the total contribution to the integral is zero.

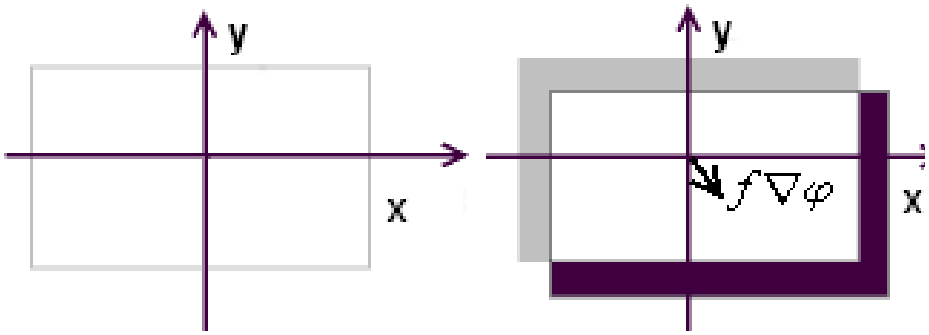

Fig. 2: (Left) a schematic drawing of the integration range Ξ. (Right) the effective support of the integral, $A_{\Xi}(\bar{r}) - A_{\Xi - f\nabla\varphi}(\bar{r})$. In the black area the function has a value of -1, in gray a value of 1, and the area in white is where the function vanishes. As the duty cycle tends to zero, the contribution of the integrand becomes negligible over these regions until at the limit, the integral vanishes.

More formally, this can be shown using the results obtained by Teague for the first moment of the Fresnel diffraction [19]: the centroid at the image plane can easily be calculated if the intensity and the phase are known at the aperture plane:

$$\langle \bar{r} \rangle = f \iint_{AP} I(\bar{r}_1) \nabla\varphi(\bar{r}_1) d^2 r_1 \Big/ \iint_{AP} I(\bar{r}_1) d^2 r_1 \quad (6).$$

Here, the integration is carried over the whole aperture. However, this formula correlates to a centroid taken over the whole image plane. In our case the phase gradient is assumed to constant over the whole aperture and thus can be

taken outside of the integral. Combining **Error! Reference source not found.** and **Error! Reference source not found.** we can now write

$$f\nabla\varphi+\lim_{\Xi\to\mathbb{R}^2}\bar{\Delta}_{\Xi}=f\nabla\varphi\iint_{AP}I(\bar{r}_1)d^2r_1\Big/\iint_{AP}I(\bar{r}_1)d^2r_1 \quad (7),$$

and so we conclude that $\lim_{\Xi\to\mathbb{R}^2}\bar{\Delta}_{\Xi}=0$.

3. EM field with spatially slow change in phase and amplitude, inside round aperture

We next investigate the behavior of the centroid operator when the duty cycle of the PSF is finite, namely when the spot size is not very small when compared with the tile size. To do this we will calculate the intensity function in case the aperture function of the lenslet is given by $P(\bar{r}_1)=circ_R(\bar{r}_1)$, namely 1 inside a circle of radius *R* and 0 outside of it. We will further assume that the change in amplitude over each lenslet is small. Under these assumptions we may take the first order Taylor approximation for the field amplitude. We narrow the definition of the EM field at the aperture according to these constraints.

$$U_1(\bar{r})=\gamma\int_{-\infty}^{\infty}\int_{-\infty}^{\infty}circ_R(\bar{r}_1)(A_0+\nabla A\cdot\bar{r}_1)exp(-i\alpha\bar{r}\cdot\bar{r}_1)d\bar{r}_1 \quad (8)$$

A_0 and ∇A are the values of the amplitude and of the amplitude gradient, evaluated at the center of the subaperture. This treatment is very similar to dipole expansion for a pair of electric point sources, and the resulting intensity (as will be shown herein) will also bear a strong resemblance to dipole energy of two displaced point sources.

We now have

$$U_1^{S}(\bar{r})=\gamma\int_{-\infty}^{\infty}\int_{-\infty}^{\infty}A_0circ_R(\bar{r}_1)exp(-i\alpha\bar{r}\cdot\bar{r}_1)d\bar{r}_1 \quad (9)$$

and

$$U_1^{AS}(\bar{r})=\gamma\int_{-\infty}^{\infty}\int_{-\infty}^{\infty}circ_R(\bar{r}_1)\nabla A\cdot\bar{r}_1\,exp(-i\alpha\bar{r}\cdot\bar{r}_1)d\bar{r}_1 \quad (0).$$

U_1^{S} is the Fresnel pattern of a wave of constant amplitude propagating along the *z* axis, and passing through a round aperture. This is the unperturbed pattern, and its associated intensity is the well known Airy pattern. In polar

coordinates the solution is given by $U_1^S(r,\xi)=\gamma\pi R^2 A_0\left[2J_1(\alpha Rr)/\alpha Rr\right]$ where J_1 is a Bessel function of the first kind with index 1. ξ is the angle from the origin in the image plane (Fig. 1).

Now let us calculate $U_1^{AS}(\overline{r})$. First we write $U_1^{AS}(\overline{r})$ in polar coordinates.

$$\begin{aligned}&\nabla A\cdot\overline{r_1}=|\nabla A|\,r\cos(\theta-\psi)\\&=|\nabla A|\,r\left[C\cos(\theta-\xi)-S\sin(\theta-\xi)\right]\end{aligned}\quad(11)$$

ψ is the direction of the gradient of A, ξ is the direction of $\overline{r}$ in the image plane and θ is the direction of the integration variable $\overline{r_1}$ in the aperture plane (Fig. 1). $C=\cos(\xi-\psi)$ and $S=\sin(\xi-\psi)$. We can now write

$$\begin{aligned}&U_1^{AS}(r,\xi)=\\&\gamma|\nabla A|\int_0^R r^2\int_0^{2\pi}\left[\cos(\theta-\xi)C-\sin(\theta-\xi)S\right]\\&\times\exp\left[-i\alpha rr_1\cos(\theta-\xi)\right]dr_1d\theta\end{aligned}\quad(12)$$

Using a Bessel function identity [20]

$$J_n(x)=\frac{1}{\pi i^{3n}}\int_0^{\pi}\cos(n\theta)\exp(-ix\cos\theta)\,dr d\theta,$$

it can easily be shown that

$$\begin{aligned}&C\int_0^{2\pi}\cos(\theta-\xi)\exp\left[-i\alpha rr_1\cos(\theta-\xi)\right]d\theta\\&=-i2\pi\cos(\xi-\psi)J_1(\alpha rr_1)\end{aligned}\quad.(13)$$

Taking the derivative of

$$S\int_0^{2\pi}\sin(\theta-\xi)\exp\left[-i\alpha rr_1\cos(\theta-\xi)\right]d\theta$$

with respect to r and then using symmetry considerations, it can easily be shown that

$$\int_0^{2\pi}\sin(\theta-\xi)\exp\left[-i\alpha rr_1\cos(\theta-\xi)\right]d\theta=0\ .\quad(14).$$

So we can carry on with the integration by r. Using the Bessel function identity $\int r^2J_1(r)\,dr=r^2J_2(r)$ [21], we have:

$$U_1^{AS}(r,\xi)=-i2\pi R^3\gamma\cos(\xi-\psi)|\nabla A|\,J_2(\alpha Rr)/(\alpha Rr).\quad(15)$$

Let us define $\bar{\beta} = \alpha R(\bar{r} - f\nabla\varphi)$ and $\beta = |\bar{\beta}|$. We can now write the full displaced diffraction pattern including the perturbation term:

$$U(\bar{r}) = \gamma\pi R^2 A_0 \left\{ J_1(\beta)/\beta - \left[i\left(R\nabla A/A_0\right)\cdot \bar{\beta}/\beta \right] J_2(\beta)/\beta \right\}$$

The corresponding intensity is

$$I(\bar{r}) = I_0 \left[\frac{J_1^2(\beta)}{\beta^2} - i\varepsilon \cos^2(\psi - \xi') \frac{J_2^2(\beta)}{\beta^2} \right] \quad , (16),$$

where $I_0 = \left(\pi R^2 A_0 / \lambda f\right)^2$ and $\varepsilon = \left(R\nabla A/A_0\right)^2$. ξ' is the direction of $\bar{\beta}$ in the image plane (Fig. 1).

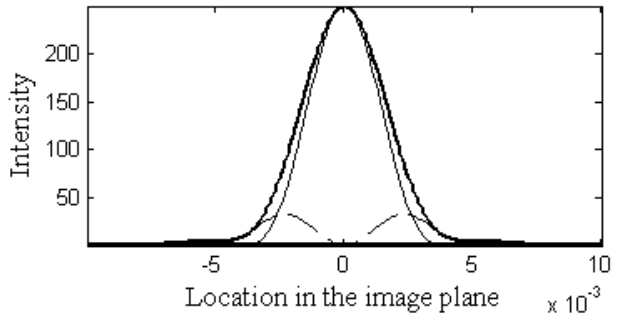

Fig. 3: The full intensity $I(\bar{r})$ (bold line) decays more slowly when the perturbed intensity $I_2(\bar{r})$ (dot-dash line) is added to it relative to the case of $I_1(\bar{r})$ in which it is absent (full line).

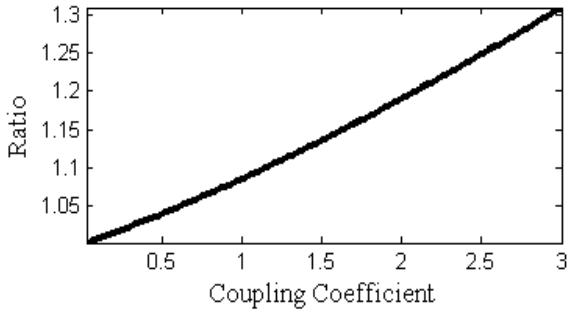

Fig. 4: The standard deviation ratio $std\left[I_1(\bar{r}) + I_2(\bar{r})\right] / std\left[I_1(\bar{r})\right]$ as a function of the coupling coefficient ε at a fixed duty cycle. As ε is increased, the standard deviation of the intensity increases, making the centroid operator more susceptible to distortion in finite duty cycles.

4. Centroid operator of a wavefront with spatially slow phase, at finite duty cycle

We recognize the first term $I_1(\bar{r}) = I_0 J_1^2(\beta)/\beta^2$, as the unperturbed, shifted intensity and $I_2(\bar{r}) = I_0 \varepsilon cos^2(\psi - \xi') J_2^2(\beta)/\beta^2$ as the perturbed, shifted intensity. It is interesting to compare the perturbation term with the unperturbed term: in I_1 we have $J_1^2(\beta)/\beta^2$ whereas in I_2 this is replaced by $J_2^2(\beta)/\beta^2$. This is significant because it means that the unperturbed term has a maximum at $\beta = 0$ but the perturbed term does not. $J_2^2(\beta)/\beta^2$ has a maximum on a ring some distance away from $\beta = 0$. A cross cut of the intensity functions in shown in Fig. 3. ε is

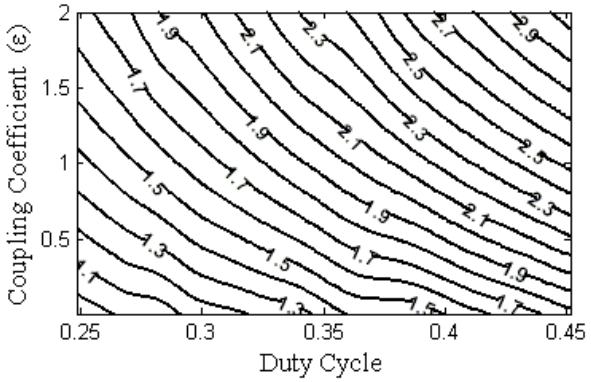

Fig. 5: The ratio of the centroid distortion to its signal, $\|\bar{\Delta}_\Xi\|/\|f\nabla\varphi\|$, as a function of the duty cycle and of the coupling coefficient ε of the perturbation term. The relative distortion increases with the ε , and with duty cycle. Significantly, sensitivity to change in ε is enhanced as the duty cycle becomes higher.

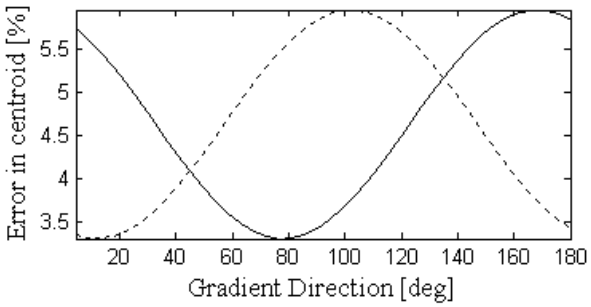

Fig. 6: The induced error to signal ratio, $\bar{\Delta}_\Xi/\|f\nabla\varphi\|$, for the diffraction pattern centroid, as the direction of the amplitude gradient is changed but the amplitude gradient size, phase gradient and duty cycle are kept constant. The solid line is the error of the *x* component and the dashed for the *y* component. It is seen that the direction of the amplitude gradient has a significant effect on the error.

the relative amplitude stroke over the aperture. It is a dimensionless term and can be thought of as a coupling constant. So as ε increases, the relative effect of the perturbation with respect to the unperturbed pattern is enhanced. The perturbed term has a larger standard deviation than the unperturbed term (Fig. 3 and Fig. 4). As the perturbation becomes more dominant (while keeping a constant duty cycle) the standard deviation of the intensity increases, making it more susceptible to error. When the duty cycle is increased, the distortion becomes more severe. This behavior is exacerbated as the amplitude variation becomes more dominant over the aperture plane (Fig. 5). There is a difference in the symmetry of the two terms: the perturbed term I_2 is symmetrical under the parity operator, but does not have full radial symmetry as the unperturbed term does. The error induced when the duty cycle is finite is thus dependent also on the amplitude gradient, both on its direction and on its magnitude (Fig. 6.).

5. Conclusions

In this paper we formulated the distortion of the centroid operator $\bar{\Delta}_{\Xi}$ of the intensity pattern in the image plane over an integration area, under the assumption that the wavefront phase is spatially slow. It was then shown that the distortion of the centroid operator approaches zero as the duty cycle of the diffraction spot approaches zero, in agreement with [18]. There it was shown that the distortion does not manifest itself when the wavefront phase gradient over the aperture is constant. The model described there is constrained to a centroid operator over the whole image plane – in effect a zero duty cycle. In practice, we are often interested in measuring the centroid when the tile is finite. This is certainly true for the HSS.

The distortion of the centroid operator taken over a finite tile was then investigated for a case in which the intensity variation is also slow in space, and the aperture is round. It was found that in this case distortion is present even if the wavefront phase gradient is constant over the whole aperture, as was discussed in [10], and that this distortion becomes progressively worse as the duty cycle increases. It was shown that when an amplitude variation over the aperture is present, the distortion becomes dependent not only on the phase gradient and duty cycle as was the case in [10], but also on the amplitude gradient magnitude and direction, thus making it computationally harder to compensate for it in real time applications. As the duty cycle increases, the centroid operator is more susceptible to distortion in the case of varying amplitude, relative to the case in which the amplitude is kept constant. Using larger lenslets in the HSS, as was discussed in [18], would on the one hand exacerbate the distortion due to a larger variation in amplitude over the aperture plane. On the other hand the duty cycle would become smaller. As was shown in this

paper this would have the effect of alleviating the distortion. So using lenslets that are excessively small or excessively large has the effect of deteriorating the performance of the centroid operator. For specific tasks, detailed planning must be carried according to specific requirements, such as expected wavefront distortion scale, number of photons, diameters of lenslets necessary, and detector characteristics (number of available pixels, well depth, noise type, etc).

Applications of the theory developed here go far beyond wavefront sensing. There are many devices which use a centroid location following a lens or an aperture, namely analogue and digital position sensors. These can be found in automated tracking systems, in disk drive writers, in compact disk players, and many more. Our calculation holds also if the size of the pixels sampling the light distribution is larger than the diffraction limit (in which some aliasing of the wavefront slopes might occur).

References

1. R. K. Tyson, *Principles of Adaptive Optics, 2nd ed.* (Academic Press, 1998)
2. D. G. Sandler, L. Cuellar, M. Lefebvre, T. Barrett, R. Arnold, P. Johnson, A. Rego, G. Smith, G. Taylor, and B. Spivey, "Shearing interferometry for laser-guide-star atmospheric at large D/r,". J. Opt. Soc. Am. A **11**, 858-873 (1994)
3. R. H. Hudgin, "Wave-Front reconstruction for compensated imaging," J. Opt. Soc. Am. **67**, 357-378 (1977)
4. D. L. Fried, "Least-Square fitting of a wave-front distortion estimate to an array of phase difference measurements." J. Opt. Soc. Am **67,** 370-375 (1977)
5. W. H. Southwell, "Wave Front estimation from wave front slope measurememts," J. Opt. Soc. Am. **70,** 998-1006 (1980)
6. A. Talmi, and E. N. Ribak, "Wavefront reconstruction from its gradients," J. Opt. Soc. Am. A **23**, 288-297 (2006)
7. K. Freischlad, and C. L. Koliopoulos, "Modal estimation of a wave front from difference measurements using the discrete Fourier transform,", J. Opt. Soc. Am. A **3** 1852–1861 (1986).
8. A. Talmi, and E. N. Ribak, "Direct demodulation of Hartmann-Shack patterns," J. Opt. Soc. Am. A **21**, 632-639 (2004).
9. Y. Carmon, and E. N. Ribak, "Phase retrieval by demodulation of a Hartmann–Shack sensor," Opt. Comm. **215**, 285-288 (2002).

10. M. A. Van Dam, and R. G. Lane, "Wave-front slope estimation," J. Opt. Soc. Am. A **17**, 1319-1324 (2000).

11. T. Berkefeld , D. Soltau and, and O. von der Luhe, "Multi-conjugate adaptive optics at the Vacuum Tower Telescope, Tenerife", Proc. SPIE **4839**, 66-76 (2002).

12. P. M. Prieto, F. Vargas-Martı´n, S. Goelz, and P. Artal, "Analysis of the performance of the Hartmann–Shack sensor in the human eye," J. Opt. Soc. Am. A **17**, 1388-1398 (2000).

13. H. J. Hofer, P. Artal, B. Singer, J. L. Aragón, and D. R. Williams "Dynamics of the eye's wave aberration", J. Opt. Soc. Am. A **18,** 497 (2001).

14. J. Primot, "Theoretical description of Shack-Hartmann wave-front sensor," Opt. Commun **222**, 81-89 (2003).

15. E. N. Ribak, and E. Gershnik, "Light propagation through multilayer atmospheric turbulence," Opt. Commun **142**, 99-105. (1997).

16. N. Saga, K. Tanaka, and O. Fukumitsu, "Diffraction of a Gaussian beam through a finite aperture lens and the resulting heterodyne efficiency," Appl. Opt. **20**, 2827–2831 (1981).

17. K. Tanaka, and O. Kanzaki, "Focus of a diffracted Gaussian beam through a finite aperture lens: experimental and numerical investigations," Appl. Opt. **26**, 390–395 (1987).

18. S. Bara**,** "Measuring eye aberrations with hartmann-shack wave-front sensors: Should the irradiance distribution across the eye pupil be taken into account?" J. Opt. Soc. Am. A **20**, 2237-2245 (2003).

19. M. R. Teague, "Irradiance moments: their propagation and use for unique retrieval of phase*,*″ J. Opt. Soc. Am. A **72**, 1199-1209 (1982).

20. A. Gray, and G. B. Mathews, *A treatise on Bessel functions and their applications in physics second edition* (Dover, 1922), pp. 43.

21. F. E. Relton, *Applied Bessel functions* (Dover, 1946), pp. 55.